Biochimica et Biophysica Acta 1840 (2014) 1771–1781

Contents lists available at ScienceDirect

Biochimica et Biophysica Acta

journal homepage: www.elsevier.com/locate/bbagen

# Iron uptake and transfer from ceruloplasmin to transferrin

Chantal Eid, Miryana Hémadi, Nguyêt-Thanh Ha-Duong *, Jean-Michel El Hage Chahine *

*Université Paris Diderot, Sorbonne Paris Cité, CNRS, Interfaces, Traitements, Organisation et Dynamique des Systèmes, UMR 7086, Bâtiment Lavoisier, 15 rue Jean-Antoine de Baïf, 75205 Paris Cedex 13, France*

ARTICLE INFO

*Article history:*
Received 17 October 2013
Received in revised form 19 December 2013
Accepted 3 January 2014
Available online 11 January 2014

*Keywords:*
Iron-metabolism
Multi-copper oxidase
Metal-transport
Aceruloplasminemia
Protein–protein adduct

ABSTRACT

*Background:* Dietary and recycled iron are in the $Fe^{2+}$ oxidation state. However, the metal is transported in serum by transferrin as $Fe^{3+}$. The multi-copper ferroxidase ceruloplasmin is suspected to be the missing link between acquired $Fe^{2+}$ and transported $Fe^{3+}$.
*Methods:* This study uses the techniques of chemical relaxation and spectrophotometric detection.
*Results:* Under anaerobic conditions, ceruloplasmin captures and oxidizes two $Fe^{2+}$. The first uptake occurs in domain 6 (<1 ms) at the divalent iron-binding site. It is accompanied by $Fe^{2+}$ oxidation by $Cu^{2+}_{D6}$. $Fe^{3+}$ is then transferred from the binding site to the holding site. $Cu^{+}_{D6}$ is then re-oxidized by a $Cu^{2+}$ of the trinuclear cluster in about 200 ms. The second $Fe^{2+}$ uptake and oxidation involve domain 4 and are under the kinetic control of a 200 s change in the protein conformation. With transferrin and in the formed ceruloplasmin–transferrin adduct, two $Fe^{3+}$ are transferred from their holding sites to two C-lobes of two transferrins. The first transfer (~100 s) is followed by conformation changes (500 s) leading to the release of monoferric transferrin. The second transfer occurs in two steps in the 1000–10,000 second range.
*Conclusion:* $Fe^{3+}$ is transferred after $Fe^{2+}$ uptake and oxidation by ceruloplasmin to the C-lobe of transferrin in a protein–protein adduct. This adduct is in a permanent state of equilibrium with all the metal-free or bounded ceruloplasmin and transferrin species present in the medium.
*General significance:* Ceruloplasmin is a go-between dietary or recycled $Fe^{2+}$ and transferrin transported $Fe^{3+}$.


## 1. Introduction

Both dietary and recycled iron are in the $Fe^{2+}$ oxidation state [1,2]. However, the metal is transported in serum by the iron-transport protein, transferrin (T) in the $Fe^{3+}$ oxidation state [1,3]. This implies the existence of a mediator capable of taking charge of the acquired and recycled $Fe^{2+}$ in order to deliver it as $Fe^{3+}$ to transferrin. During this process, iron, in its two oxidation states, should never be allowed to enter into contact with the aqueous biological environment. Indeed, both oxidation states are involved in Fenton and Haber–Weiss chemistries. These are responsible for generating highly reactive oxygen radicals that cause irreversible damage to cells and their environment [2,4,5]. Ceruloplasmin (Cp) is strongly suspected of being this mediator which can play the role of an antioxidant inhibiting free radical formation [6–9]. Another hypothesis envisages a $Fe^{2+}$ capture by T and its oxidation to $Fe^{3+}$ once bound because of the strongly negative redox potential (−500 mV at pH 5.6) for iron in the protein [10].

Human serum ceruloplasmin (Cp) is a multifunctional glycoprotein that carries 95% of the plasma copper in mammals [11]. This protein oxidizes a number of structurally unrelated molecules, such as 4-phenylenediamine, amino-phenols, catechols and 5-hydroxyindoles and even nitric oxide [12–15]. However, its main activity is assumed to be that of ferroxidase. This assumption is confirmed by the facts that humans with mutations of the ceruloplasmin gene (aceruloplasminemia) show iron accumulation in several organs including the retina, liver and brain [16]. This loss of the ferroxidase activity leads to the accumulation of an excess of iron in the liver, spleen and pancreas of pigs and rodents, as well as in ceruloplasmin knockout mice [17–21]. Cp is a 132 kDa enzyme that consists of a single polypeptide chain of 1046 amino acids folded in six domains [22–24]. It is a member of the multi-copper oxidase family that comprises ascorbate oxidase and the laccases [25]. These enzymes are characterized by three types of copper-binding sites [26]. In Cp there are three type 1 coppers, which are responsible for its typical blue color, with an absorption maximum, $\lambda_{Cp} = 610$ nm. The type 1 occupies a distorted tetrahedral site which is shaped by two histidines, one cysteine along with one methionine, or more rarely, a leucine [27]. Furthermore, three other coppers are engaged in a cluster, in which a pair of type 3 copper atoms are attached to a type 2 site [28]. The trinuclear coordination site consists of four pairs of histidine. The two type 3 (T3) copper are bound to six histidines and constitute a pair of antiferromagnetically coupled copper ions, whereas the type 2 (T2) copper is coordinated by two histidines. A dioxygen is bound to the trinuclear copper cluster [29].

*Abbreviations:* Cp, ceruloplasmin; T, apotransferrin; Cp-T, ceruloplasmin–transferrin protein–protein adduct; $Cu_{D6}$, type 1 copper of domain 6 in Cp; $Cu_T$, type 3 copper of the trinuclear cluster of Cp; $Cu_{D4}$, type 1 copper of domain 4; $TFe_2$, holotransferrin; $T_CFe$, $T_CFe\text{-}T_N$, $TFe^{3+}$ C-lobe monoferric transferrin; GSH, reduced glutathione

* Corresponding authors. Tel.: +33 157277239, +33 157277238; fax: +33 157277263.
*E-mail addresses:* thanh.haduong@univ-paris-diderot.fr (N.-T. Ha-Duong), chahine@univ-paris-diderot.fr (J.-M. El Hage Chahine).

0304-4165/$ – see front matter © 2014 Elsevier B.V. All rights reserved.
http://dx.doi.org/10.1016/j.bbagen.2014.01.011

The cluster is sufficiently close to the type 1 (T1) coppers to allow an electron transfer between the latter and the trinuclear center. This provides for the reduction of the dioxygen and the release of two water molecules without any liberation of reactive oxygen species [30,31].

Transferrin is a glycoprotein of 700 amino-acids organized in two semi-equivalent lobes, each of which contains an iron-binding site composed of two phenols of two tyrosines, a carboxylate of an aspartate, an imidazole of a histidine and a synergistic carbonate adjacent to an arginine. The apo-form (iron-free) is in the so-called open conformation where the protein ligands are in direct contact with the bulk medium. In the iron-loaded transferrin or holotransferrin ($TFe_2$), each lobe encloses the coordinated metal, which becomes buried about 10 Å under the surface of the protein in a closed conformation [32–34]. T has a very high affinity for $Fe^{3+}$ ($10^{21}$) and a much lower one for $Fe^{2+}$ ($\sim 10^7$) [35,36]. $TFe_2$ interacts extremely rapidly with transferrin receptor 1, which is anchored in the plasma membrane [37]. The two proteins in interaction are then internalized in the cytoplasm by receptor-mediated endocytosis [38].

$Fe^{3+}$ is basically insoluble in aqueous neutral media, where it readily precipitates as different iron hydroxide species. $Fe^{3+}$ is usually solubilized in the form of low-molecular-mass chelates or complexed to proteins or macromolecules. In the normal individual about 0.1% of the total body iron (i.e. about 3 to 4 mg) is in the plasma, bound predominantly to transferrin (which is approximately 30% saturated with iron). The daily turnover of iron is about 30 mg. Thus, transferrin is continually binding iron (both dietary and recycled iron) and delivering it to cells and tissues [2,3,39,40]. We established a few years ago the mechanisms of $Fe^{3+}$ uptake by transferrin from soluble complexes, and showed that these processes occur in several kinetic steps ranging from milliseconds to hours [41,42]. The concentration of non-transferrin-bound iron in the serum ($\leq$0.1 mg) is extremely low [2,43,44]. This, added to the rates we reported for $Fe^{3+}$ uptake by transferrin from chelates, is far from sufficient for the required iron turnover. How, then, is iron acquired by transferrin, and is Cp involved?

We recently showed that Cp interacts with both apo- and holotransferrin with a dissociation constant of about 15 μM [45]. These interactions are extremely weak as compared to that of $TFe_2$ or the C-lobe-only iron-loaded transferrin ($T_CFe\text{-}T_N$) with receptor 1 (2.3 nM) [37,46]. Cp cannot, therefore, interfere with the recognition of $TFe_2$ by the receptor. In the blood stream the concentrations of Cp (2.5 μM) and transferrin (25 μM) [47,48], imply that 70% of the circulating Cp is interacting with transferrin [45]. However, this does not provide any evidence for a transfer of $Fe^{3+}$ from Cp to T.

The work presented here consists of two essential parts. In the first, we analyze $Fe^{2+}$ uptake by Cp and revisit its oxidation to $Fe^{3+}$. In the second, we research the possibility of an intramolecular $Fe^{3+}$ transfer from Cp to T in the Cp–T protein–protein adduct. These investigations are based on the use of chemical relaxation and spectrophotometric techniques [49,50].

## 2. Material and methods

### 2.1. Material

Apotransferrin was purchased from Sigma, and purified according to published procedures [41]. Ceruloplasmin was purchased from Euromedex, and used without further purification. The copper load was checked as described elsewhere [51]. Commercial ceruloplasmin carries 5 $Cu^{2+}$ and 2 $Cu^{+}$ and is iron-free. KCl (Merck Suprapur), NaOH, HCl (Merck Titrisol), $NaHCO_3$, HEPES (2-[4-(2-hydroxyethyl)piperazin-1-yl] ethanesulfonic acid), sodium ascorbate, $Fe(NH_4)_2SO_4 \cdot 6H_2O$ (Fluka) and reduced glutathione (Sigma) were of the purest possible grades.

#### 2.1.1. Stock solutions

The HEPES concentration in neutral buffers was 50 mM. Final pHs were continuously controlled and adjusted to between 6.6 and 8.6 with micro-quantities of concentrated HCl or NaOH. Cp concentrations ($c_1$) were checked by a Bio Rad protein assay and spectrophotometrically [52]. Final solutions of Cp and T ($c_2$) were diluted further to the required concentrations in the buffers. $c_1$ varied from 50 nM to 5 μM and $Fe^{2+}$ concentrations ($c_3$) from 15 to 1000 μM. All final ionic strengths were adjusted to 0.2 M with KCl.

Crystalline ferrous ammonium sulfate hexahydrate, $Fe(NH_4)_2SO_4 \cdot 6H_2O$, was used as the ferrous iron source and was dissolved at 10 mM in a 0.2 M deoxygenated KCl solution. Ferrozine (3-(2-pyridyl)-5,6-bis(4-phenylsulfonic acid)-1,2,4-triazine) was dissolved at 2.5 mM in 0.1 M NaCl. Sodium ascorbate ((2*R*)-2-[(1*S*)-1,2-dihydroxyethyl]-4-hydroxy-5-oxo-2*H*-furan-3-olate) and reduced glutathione were dissolved in deoxygenated 50 mM Hepes, 20 mM $NaHCO_3$, and 130 mM KCl buffer.

### 2.2. Methods

#### 2.2.1. pH measurements

pH values were measured in a glove box with a Jenco pH-meter equipped with a "Metrohm" combined calomel/glass mini-electrode. The pH-meter was standardized at working temperature by standard buffers: pH 7.00 and 10.01 (Beckman). At the end of the measurements, pHs were double-checked both in the buffer and in the protein solutions. They were accurate to better than 0.02 pH unit.

#### 2.2.2. Spectrophotometric measurements

Absorption measurements were performed at (25 ± 0.1) or (10 ± 0.1) °C on a Cary 4000 spectrophotometer equipped with a Peltier thermostated cell-carrier. Fluorimetric measurements were performed at (25 ± 0.1) or (10 ± 0.1) °C on a Fluorolog 3 Horriba Jobin-Yvon equipped with a thermostated cell-carrier. Emission spectra were measured in the 300–400 nm range. Excitation wavelength was set to 280 nm. The spectra used for equilibrium constants determinations were recorded at the final equilibrated state. The cuvettes had a capacity of 100 or 1000 μL. They were especially designed to be used under anaerobic conditions and were, when required, manipulated in a glove box before being transferred to the spectrometers (transfer time about 2 min).

#### 2.2.3. Ferroxidase activity

Ferroxidase activity was measured with ferrous ammonium sulfate as substrate, in 50 mM HEPES, 20 mM $NaHCO_3$, 130 mM KCl, pH between 6.6 and 8.5 at 10 and 25 °C. Cp (50 nM) was incubated with ferrous iron solution ($10^{-7}$–$10^{-3}$ M). Aliquots were removed at specific time intervals and added to 2.5 mM of ferrozine solution, which stopped the enzymatic reaction and allowed the detection of the ferrous-ferrozine complex ($\varepsilon_{562} = 27\,900\ M^{-1}\ cm^{-1}$) [53].

#### 2.2.4. Dissociation constants of Cp–Fe complexes

Dissociation constants were determined spectrophotometrically by the use of the Global Analysis program SPECFIT 32. SPECFIT is a multivariate data analysis program for data sets that are obtained from multiwavelength spetrophotometric measurements. The program utilizes a specially adapted version of the Levenberg–Marquardt method. This procedure returns optimized model parameters, their standard errors, and the predicted spectra of the unknown colored species [54]. The dissociation constants were checked when possible by a variant of the Benesi and Hildebrand method [45].

#### 2.2.5. Kinetics

Stopped-flow experiments were performed under anaerobic conditions by mixing solutions of ceruloplasmin or ceruloplasmin–apotransferrin with $Fe^{2+}$ on a Hi-Tech Scientific SF61DX2 stopped-flow spectrophotometer equipped with a Xe/Hg light source and a thermostated bath held at 10 or 25 °C. The mixing syringes, reservoirs and chambers were kept under argon in a specially designed box. The solutions were prepared in a glove box and introduced by syringes kept under argon in

their respective reservoirs by injection though a rubber septum. All signals were accumulated at least 10 times. In fluorimetric experiments, the excitation wavelength was usually set at 280 nm. However, for stopped-flow, the excitation wavelength was set 295 nm, which is one of the emission peaks of the Xe/Hg light source, and detection was set at $\lambda_{em} \geq 320$ nm.

## 3. Results

The $Fe^{2+}$ donor to Cp used in our experiment was ferrous ammonium sulfate in the absence or presence of reduced glutathione (GSH). All the solutions were deoxygenated, and the experiments were performed under anaerobic conditions in a glove box under argon. Spectrophotometric detection was used in all thermodynamic and kinetic runs. The kinetic processes related to $Fe^{2+}$ uptake by Cp were acquired by fluorescence emission and absorption ($\lambda = 610$ nm). Those related to iron-transfer from Cp to T were acquired by absorption at $\lambda = 465$ nm and/or 610 nm. The charge of the protein species is not indicated.

### 3.1. Iron(II) binding

Under anaerobic conditions, adding $Fe^{2+}$ to a solution of Cp led to a decrease in the fluorescence emission accompanied by a 6 nm red-shift (from 331 to 337 nm) (Fig. 1). A SPECFIT analysis showed that two $Fe^{2+}$ complexes are produced sequentially with Cp (Eqs. (1) and (2)).

$$Cp + Fe^{2+} \rightleftharpoons CpFe \quad (1)$$

$$CpFe + Fe^{2+} \rightleftharpoons CpFe_2 \quad (2)$$

with

$$K_{d1} = \frac{\left[Fe^{2+}\right][Cp]}{[CpFe]}; \quad K_{d2} = \frac{\left[Fe^{2+}\right][CpFe]}{[CpFe_2]};$$

$K_{d1}$ and $K_{d2}$ are independent of pH in the 6.5–8.5 pH range. They were measured at two different temperatures: 25 °C, $K_{d1} = 5.5 \pm 2.5$ μM and $K_{d2} = 150 \pm 50$ μM; and 10 °C, $K_{1d} = 1.1 \pm 0.2$ μM and $K_{d2} = 150 \pm 50$ μM. These values were confirmed by a Benesi and Hildebrand analysis [45].

#### 3.1.1. Kinetics of iron(II) uptake

When a solution of Cp is mixed with a solution of $Fe^{2+}$, several kinetic processes are observed. However, at 25 °C, the first of these processes is much too fast (<10 ms) to be analyzed by the stopped-flow mixing techniques. Consequently the kinetic runs were performed at 10 °C.

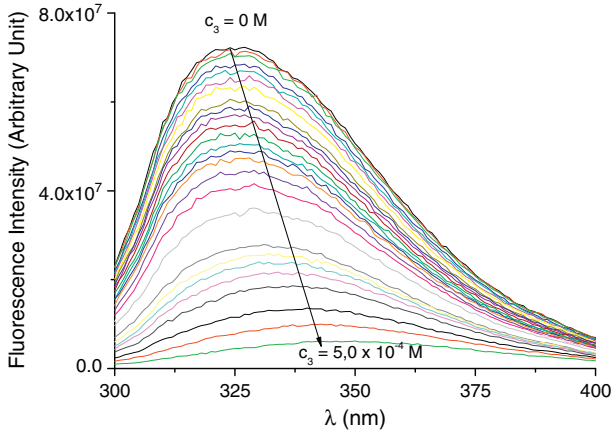


**Fig. 1.** Emission spectra of a ceruloplasmin solution ($c_1 = 0.61$ μM) at different [$Fe^{2+}$] ($0 \leq c_3 \leq 0.5$ mM) at pH 7.40, 10 ± 0.1 °C, and $\mu = 0.2$ for an excitation wavelength, $\lambda_{ex} = 280$ nm.

At 10 °C, when a solution of Cp is mixed with a solution of $Fe^{2+}$, four kinetic processes are observed (Fig. 2). The first is very fast and occurs in the millisecond range as a sharp decrease in the absorbance at $\lambda = 610$ nm (Fig. 2A). The second occurs as an exponential increase in the fluorescence in the tens of millisecond range to yield a kinetic product (Fig. 2B). The third is seen as a second exponential increase in absorption and fluorescence occurring in about 200 ms (Fig. 2A, C). These two processes are followed by a fourth exponential decrease in emission and absorbance in the 300 s range (Fig. 2D, E). The experimental reciprocal relaxation times related to the second process (Fig. 2B) depend on $Fe^{2+}$ concentration and are independent of the other experimental parameters (pH, ionic strength, Cp concentration, $c_1$). The other processes (Fig. 2C, D, E) seem to be independent of all our experimental parameters and are not observed when Cp is iron-loaded.

*3.1.1.1. First kinetic process.* The first sharp decrease in the absorbance at 610 nm (<1 ms, Fig. 2A) is typical of the reduction of the T1 $Cu^{2+}$ of domain 6 [55,56]. We ascribed this process to $Fe^{2+}$ oxidation and to its prior uptake by the iron-labile site (Eqs. (3), (4))

$$CpCu^{2+}_{D6} + Fe^{2+} \rightleftharpoons CpCu^{2+}_{D6}Fe^{2+} \quad (3)$$

$$CpCu^{2+}_{D6}Fe^{2+} \rightleftharpoons CpCu^{+}_{D6}Fe^{3+} \quad (4)$$

with an overall dissociation constant $K_1 = \frac{\left[CpCu^{2+}_{D6}\right]\left[Fe^{2+}\right]}{\left[CpCu^{+}_{D6}Fe^{3+}\right]}$.

*3.1.1.2. Second kinetic process.* The second kinetic process is only observed by fluorescence emission detection (Fig. 2B). It is not detected by absorption at 610 nm. The reciprocal relaxation times associated with this process are independent of pH, Cp concentration ($c_1$) and ionic strength. They, however, depend on $Fe^{2+}$ concentration in a continuous but non-linear mode (Fig. 3). This process cannot therefore be ascribed to a second iron uptake. Moreover, the fact that it is not detected at 610 nm eliminates the involvement and/or the reduction of T1 $Cu^{2+}$.

In an assumption based on these observations and those in the literature [30,56], we ascribed this phenomenon to the migration of $Fe^{3+}$ from the labile site to its retention site at the surface of Cp (Eq. (5)).

$$CpCu^{+}_{D6}Fe^{3+} \underset{k_{-2}}{\overset{k_2}{\rightleftharpoons}} \left\{CpCu^{+}_{D6}Fe^{3+}\right\} \quad (5)$$

with $K_2 = \frac{\left[\left\{CpCu^{+}_{D6}Fe^{3+}\right\}\right]}{\left[CpCu^{+}_{D6}Fe^{3+}\right]} = \frac{k_2}{k_{-2}}$.

The reciprocal relaxation time equation associated with Eq. (5) can be expressed as Eq. (6) (appendix):

$$\tau_2^{-1} = \frac{k_2\left[Fe^{2+}\right]}{K_1 + \left[Fe^{2+}\right]} + k_{-2}. \quad (6)$$

Varying $K_1$ from 100 to 1000 μM with a $\Delta K_1$ step of 5 μM shows that the best linear regression of $\tau_2^{-1}$ against $[Fe^{2+}]/(K_1 + [Fe^{2+}])$ is obtained for $K_1 = 155 \pm 5$ μM (Fig. 4). From the slope and intercept, $k_2 = 32 \pm 4\ s^{-1}$, $k_{-2} = 155 \pm 5\ s^{-1}$ and $K_2 = 0.20 \pm 0.01$ were determined.

*3.1.1.3. Third kinetic process.* The third kinetic process is observed as an increase in emission and absorption at 610 nm which lasts about 200 ms (Fig. 2A, C). The reciprocal relaxation times associated with this process seem to be independent of the concentrations of the species present in the medium. This implies first-order kinetics, such as a conformation change, a tautomery, an intramolecular electron-transfer, etc. [50,57]. Furthermore, the fact that the process is associated with an increase in the absorbance at 610 nm involves the oxidation of a T1

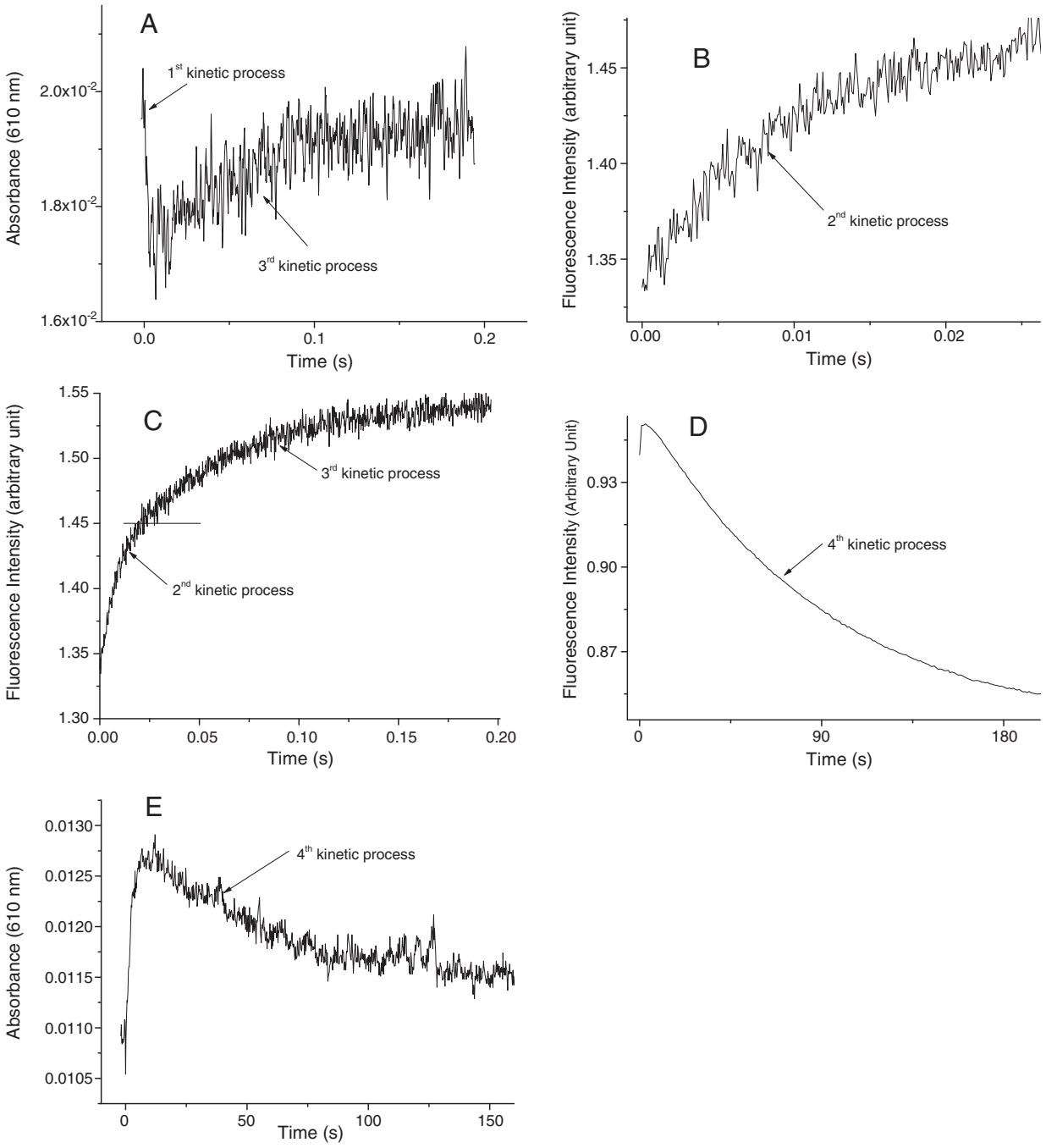


**Fig. 2.** Variation of the emission ($\lambda_{ex} = 295$ nm; $\lambda_{em} \geq 320$ nm) and absorption ($\lambda = 610$ nm) with time after a fast mixing of a ceruloplasmin solution with $[Fe^{2+}]$ at 10 ± 0.1 °C and $\mu = 0.2$; (A) and (E), $c_1 = 4$ μM, $c_3 = 0.2$ mM, pH 6.5; (B) (C) and (D), $c_1 = 0.18$ μM, $c_3 = 0.2$ mM, pH 7.3.

$Cu^{+}$ to $Cu^{2+}$ of domain 6. This led us to ascribe it to the oxidation of the $Cu^{+}_{D6}$ of $\{CpCu^{+}_{D6}Fe^{3+}\}$ by $Cu^{2+}_{T}$ of the trinuclear cluster of the protein (Eq. (7)) [30,56]. In Eq. (7), the $\{CpCu^{+}_{D6}Fe^{3+}\}$ species is expressed as $(Cu^{2+}_{T})CpCu^{+}_{D6}Fe^{3+}$.

$$\left(Cu^{2+}_{T}\right)CpCu^{+}_{D6}Fe^{3+} \underset{k_{-3}}{\overset{k_3}{\rightleftharpoons}} \left(Cu^{+}_{T}\right)CpCu^{2+}_{D6}Fe^{3+} \quad (7)$$

$$\tau_3{}^{-1} = k_3 + k_{-3} = 19 \pm 3\ s^{-1}$$

*3.1.1.4. Fourth kinetic process.* The process in Fig. 2D and E exhibits an exponential decrease in fluorescence emission or in absorbance at 610 nm. This absorption decrease implies the involvement of a T1 $Cu^{2+}$ in domain 4. The associated reciprocal relaxation times are independent of the protein and iron concentrations. However, this process is inhibited by the presence of the copper-reducing agent, ascorbate, and ceases to be observed, when Cp is iron-saturated. Furthermore, the fact that it is independent of the iron and protein concentrations leads to first-order kinetics [50]. We ascribed this fourth phenomenon to a conformation change rate-controlling a second $Fe^{2+}$ uptake by Cp and an intramolecular $Fe^{2+}$ oxidation by T1 $Cu^{2+}$ of domain 4 (Eqs. (8), (9)). The species at the end of the third kinetic process $(Cu^{+}_{T})CpCu^{2+}_{D6}Fe^{3+}$ is expressed in Eq. (8) as $CpCu^{2+}_{D4}(Fe^{3+})$.

$$CpCu^{2+}_{D4}\left(Fe^{3+}\right) \rightleftharpoons \left\{CpCu^{2+}_{D4}\left(Fe^{3+}\right)\right\} \quad \text{rate-limiting} \quad (8)$$

$$\left\{CpCu^{2+}_{D4}\left(Fe^{3+}\right)\right\} + Fe^{2+} \rightleftharpoons \left\{CpCu^{+}_{D4}\left(Fe^{3+}\right)_2\right\} \quad (9)$$

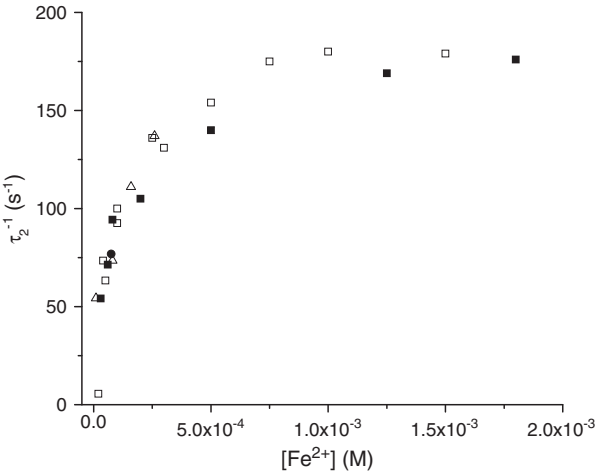


**Fig. 3.** Plot of $\tau_2^{-1}$ against [$Fe^{2+}$] at 10 ± 0.1 °C: (Δ) $c_1$ = 0.045 μM, pH 7.7; (●) $c_1$ = 0.09 μM, pH 7.3; (□) $c_1$ = 0.18 μM, pH 7.7; (■) $c_1$ = 0.18 μM, pH 7.30.

$$\tau_4^{-1} = k_4 + k_{-4} = (14 \pm 4) \times 10^{-3} s^{-1}$$

### 3.2. Iron-transfer from ceruloplasmin to transferrin

Serum apotransferrin (T) does not present any absorption spectrum above 350 nm, whereas a C-lobe-only iron-loaded ($T_CFe^{3+}$) and iron-saturated transferrin (holotransferrin, $TFe_2$) present absorption spectra between 400 and 500 nm with an absorption maximum at 465 nm related to the tyrosine-$Fe^{3+}$ complex [42]. On the other hand, as indicated above, iron-free Cp presents the typical 610 nm absorption band related to the T1 $Cu^{2+}$. These spectroscopic characteristics will be used to monitor the behavior of a mixture of these two proteins in the presence of $Fe^{2+}$. Furthermore, the experimental conditions were set so that the major species of Cp would be the ceruloplasmin–transferrin adduct (Cp–T) [45]. The affinity of T for $Fe^{3+}$ is very high, whereas that for $Fe^{2+}$ is weak [35,36]. Therefore, the slightest traces of $Fe^{3+}$ may compromise our approach. To avoid this problem, our experiments were performed in the presence of GSH. GSH is a very strong iron-reducing agent that also forms stable complexes with $Fe^{2+}$ [58,59]. Indeed, the affinity of GSH for $Fe^{2+}$ is about $10^5$ [59].

We started by comparing the ferroxidase catalytic efficiencies of Cp and that of the protein–protein Cp–T for the two iron oxidations

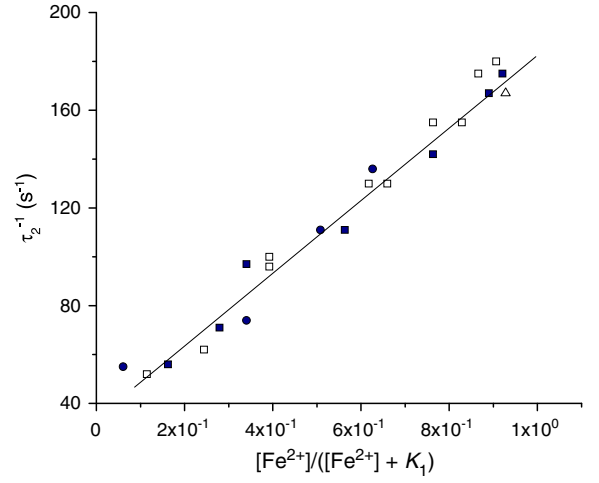


**Fig. 4.** Plot of $\tau_2^{-1}$ against [$Fe^{2+}$]/([$Fe^{2+}$] + $K_1$) with $K_1$ = 0.155 mM: (Δ) $c_1$ = 0.045 μM, pH 7.7; (●) $c_1$ = 0.09 μM, pH 7.3; (□) $c_1$ = 0.18 μM, pH 7.7; (■) $c_1$ = 0.18 μM, pH 7.3; slope, 155 ± 6 $s^{-1}$; intercept, 32 ± 4 $s^{-1}$; r = 0.98947.

($V_{M1}/K_{M1}$, $V_{M2}/K_{M2}$), where $K_{M1}$ and $K_{M2}$ are the Michaelis–Menten constants, and $V_{M1}$ and $V_{M2}$ are the maximum rates of iron oxidation catalyzed by Cp or Cp–T [60]. We show that when the Cp–T adduct is the major Cp species [45], the $V_{M1}/K_{M1}$ and $V_{M2}/K_{M2}$ values are threefold those of Cp [60]. This implies that transferrin favors kinetically the ferroxidase activity of Cp (Table 1), as the $K_M$ values remain unchanged.

In a first approach, a solution containing Cp and T in the presence of reduced glutathione (GSH), with the apoform Cp–T as the major ceruloplasmin species was mixed in the glove box with a $Fe^{2+}$ solution. The mixture was removed (in a cuvette sealed under argon) from the glove box and within 2 min after mixing (transfer time from the glove box to the spectrometer), the differential absorption spectra (where apotransferrin is the reference) were recorded between 400 and 700 nm as a function of time (1- to 2-minute intervals, Fig. 5). They implied several kinetic processes, as shown by the cuts versus time of the absorptions at 465 and 610 nm (Fig. 6).

The firsts seem to occur during the transport time from the glove box to the spectrometer. They appear as a decrease in the absorption at 610 nm accompanied by the emergence of a new absorption band at 477 nm. These processes are followed by a second increase in the absorption at 610 and 477 nm accompanied by a blue-shift from 477 to 465 nm, which in turn is followed by slow decreases in the absorbance at 465 and 610 nm. This final absorption band is typical of a $Fe^{3+}$-loaded transferrin. Therefore, several kinetic processes appear to regulate an eventual iron transfer from Cp to T.

Under our experimental conditions ([GSH] ≫ $c_1$, $c_2$, [$Fe^{2+}$]), all the $Fe^{2+}$ present in the medium is in the form of $GSHFe^{2+}$ (Eqs. (10), (11))

$$T + Fe^{2+} \rightleftharpoons TFe^{2+} \quad (10)$$

$$GSH + Fe^{2+} \rightleftharpoons GSHFe^{2+}. \quad (11)$$

#### 3.2.1. Kinetics of iron transfer from ceruloplasmin to transferrin

In order to investigate the unresolved processes that occur during transfer time from the glove box to the spectrometer (Fig. 5), stopped-flow mixing experiments were performed under anaerobic conditions (Fig. 7). When a solution containing Cp (1 μM ≤ $c_1$ ≤ 2 μM) and T (30 ≤ $c_2$ ≤ 60 μM) is rapidly mixed with a solution of $Fe^{2+}$ in the presence of reduced glutathione ($c_4$ = 5–20 mM), a first kinetic process occurs in the 100 s range as an exponential increase in absorbance at 477 nm (Fig. 7). This is followed by a second process that occurs in the 500 s range as an exponential increase in absorption with the hypsochromic shift from 477 to 465 nm (Fig. 6A). This phenomenon is also depicted by an increase in the absorption at 610 nm (Fig. 6B). The third process is a slow (about 3000 s) exponential decrease in absorbance observed at 610 nm and not at 465 nm (Fig. 6C). The fourth process is a very slow (about 10,000 s) decrease in absorbance observed at 465 nm and not at 610 nm (Fig. 6D). It should be noted here that the signal/noise ratio of our acquisition system did not allow the detection of the kinetics of the first fast and weak decrease in absorption at 610 nm (Fig. 5).

*3.2.1.1. First kinetic process.* The uptake, oxidation and transfer of iron from the binding to the holding site in domain 6 occur in less than 1 s

**Table 1**
Michaelis constants of the ferroxidase activity of Cp in the absence or presence of T (50 μM) at pH 7.2 and 37 °C.

| | In the absence of T | In the presence of T (50 μM) |
|---|---|---|
| $K_{M1}$ (M) | (5.5 ± 0.6) × $10^{-6}$ | (6.5 ± 0.9) × $10^{-6}$ |
| $V_{max1}$ ($min^{-1}$) | (0.74 ± 0.01) × $10^2$ | (2.5 ± 0.2) × $10^2$ |
| $V_{max1}/K_{M1}$ ($min^{-1} \cdot M^{-1}$) | 13.5 × $10^6$ | 38.5 × $10^6$ |
| $K_{M2}$ (M) | (0.9 ± 0.2) × $10^{-4}$ | (2.2 ± 0.6) × $10^{-4}$ |
| $V_{max2} \times 10^{-3}$ ($min^{-1}$) | (2.5 ± 0.7) × $10^3$ | (17 ± 1) × $10^3$ |
| $V_{max2}/K_{M2}$ ($min^{-1} \cdot M^{-1}$) | 27.8 × $10^6$ | 77.3 × $10^6$ |

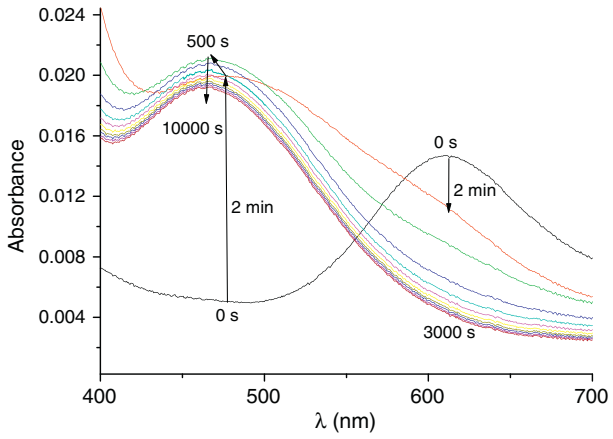


**Fig. 5.** Variation with time of the differential absorption (with reference to T) of a solution containing Cp ($c_1 = 2$ μM), T ($c_2 = 30$ μM), $Fe^{2+}$ ($c_3 = 0.12$ mM) and GSH ($c_4 = 10$ mM) at 25 ± 0.1 °C, pH 7.01 and μ = 0.2.

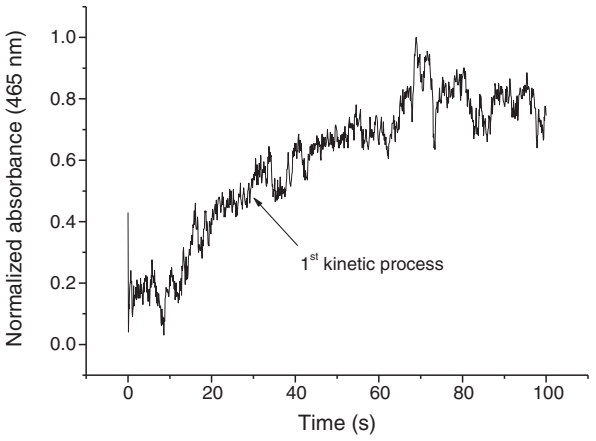


**Fig. 7.** Normalized variation of absorbance at 465 nm with time after mixing by stopped-flow a solution of Cp and T with a solution of $Fe^{2+}$ containing GSH at 25 ± 0.5 °C, pH 7.00 and μ = 0.2: $c_1 = 2$ μM, $c_2 = 30$ μM, $c_3 = 90$ μM, $c_4 = 20$ mM.

(Eqs. (4)–(6); Fig. 2A–C). Therefore, the first process in Fig. 7 is much too slow to be ascribed to these phenomena. It shows as an increase in absorption at 477 nm to yield a first kinetic product. This process is not observed when T is mixed with the $Fe^{2+}$ solution in the absence of Cp. It cannot, therefore, be ascribed to complex formation between T and $Fe^{2+}$ (Eq. (10)). $TFe^{2+}$ does not present the $Fe^{3+}$-phenate coordination responsible for the 477 nm band. This absorption can neither be related to free transferrin nor to Cp. Indeed, the absorption maximum of the iron(III) complex of transferrin is 465 nm where Cp does not absorb. Furthermore, at the end of this process and before the beginning of the second kinetic phenomena, the absorption band related to the first kinetic product at λ = 610 nm implies a reduction of T1 copper (Fig. 5), which indicates an oxidation of iron. The reciprocal relaxation times ($\tau_5^{-1}$) associated with the first kinetic process of Fig. 7 are independent

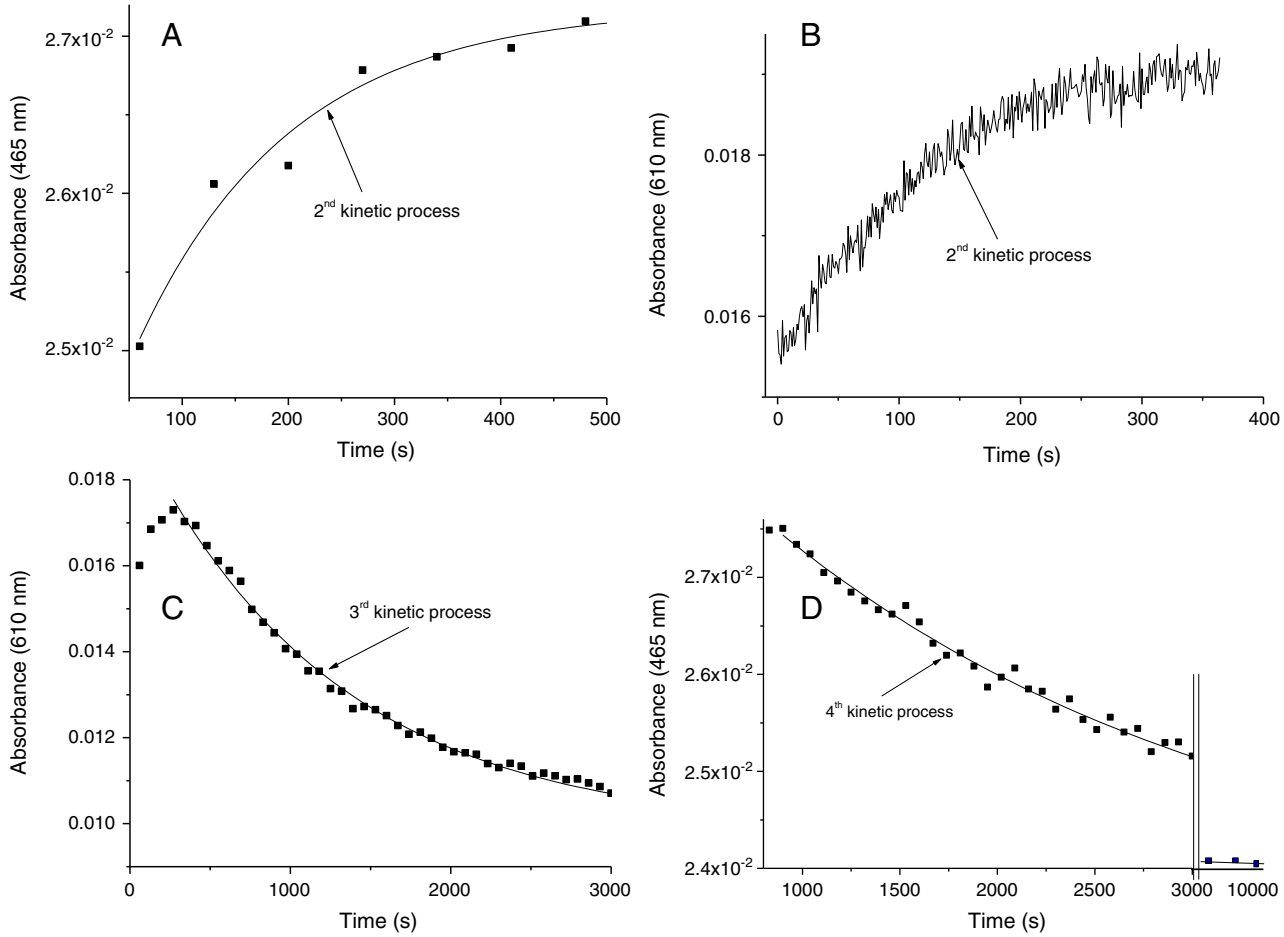


**Fig. 6.** Variation of the absorbance at 465 nm (A), (D) and 610 nm (B) (kinetic run), (C) with time after mixing a solution of Cp and T with a solution of $Fe^{2+}$ containing GSH at 25 ± 0.5 °C, pH 7.00 and μ = 0.2: (A), (C) and (D) $c_1 = 2$ μM, $c_2 = 30$ μM, $c_3 = 0.15$ mM, $c_4 = 10$ mM (C) $c_1 = 2.8$ μM, $c_2 = 50$ μM, $c_3 = 0.15$ mM, $c_4 = 5$ mM.

of the concentrations of the species present in the medium. This implies a monomolecular first-order kinetics, such as a conformation change or an intramolecular process [50,57]. We, therefore, ascribe it to a rate-limiting iron transfer from Cp to T in the Cp–T adduct following the fast iron-uptake and oxidation by Cp (Eqs. (4)–(6), (12), (13)).

$$CpFe^{3+}{-}T \underset{k_{-5}}{\overset{k_5}{\rightleftharpoons}} Cp{-}TFe^{3+} \tag{12}$$

$$\tau_5{}^{-1} = k_5 + k_{-5} = (2.2 \pm 0.2) \times 10^{-2}\mathrm{s}^{-1} \tag{13}$$

*3.2.1.2. Second kinetic process.* During the second kinetic process (Fig. 6A and B), the absorptions at 477 and 610 nm increase exponentially (identical relaxation times) in about 500 s to yield a second kinetic product that presents absorption maxima at 465 and 610 nm. The absorption maximum at 477 nm can be that of protein–protein adduct *Cp–TFe*$^{3+}$, whereas that at 465 nm is typical of $Fe^{3+}$-loaded transferrin ($T_CFe^{3+}$ or $TFe_2$). Moreover, the absorption growth at 610 nm is typical of the re-oxidation of the $Cu^{+}$ of domain 6 by a $Cu^{2+}$ of the trinuclear cluster [30,56]. The associated reciprocal relaxation times ($\tau_6^{-1}$) are independent of the concentrations of the species present in the medium. They cannot, therefore, be ascribed to the dissociation equilibrium of Cp–$TFe^{3+}$ (Eq. (14)), because in this case the reciprocal relaxation times should depend on concentrations of transferrin and Cp (Eq. (15)) [50].

$$Cp + TFe^{3+} \underset{k'_{-6}}{\overset{k'_6}{\rightleftharpoons}} Cp{-}TFe^{3+} \tag{14}$$

$$\left(\tau_6{}^{-1}\right)' = k'_6\left([\mathrm{Cp}] + \left[\mathrm{TFe}^{3+}\right]\right) + k'_{-6} \tag{15}$$

These ($\tau_6^{-1}$) imply first-order kinetics, such as an intramolecular process. In the absence of transferrin, the re-oxidation of $Cu^{+}{}_{D6}$ by the $Cu^{2+}$ of the trinuclear cluster occurs in the 200 ms range (Eq. (8), Fig. 2C). The kinetic process in Fig. 6B is, therefore, much too slow to be ascribed to Eq. (8). We ascribe it to a change in the conformation of Cp–$TFe^{3+}$ to yield a second kinetic product (Eqs. (16) and (17)). This can explain the blue shift in absorbance from 477 to 465 nm as well as the absorption increase at 610 nm.

$$Cp{-}TFe^{3+} \underset{k_{-6}}{\overset{k_6}{\rightleftharpoons}} \left(Cp{-}TFe^{3+}\right) \tag{16}$$

$$\tau_6{}^{-1} = k_6 + k_{-6} = (8.0 \pm 1.4) \times 10^{-3}\mathrm{s}^{-1} \tag{17}$$

*3.2.1.3. Third kinetic process.* The third kinetic process is detected as a slow (~3000 s) exponential decrease of the absorbance at 610 nm (Fig. 6C). Therefore, it involves again the reduction of T1 $Cu^{2+}$ and the oxidation of $Fe^{2+}$. With $c_2 \gg c_1$, apo-, iron-loaded transferrin and the protein–protein ceruloplasmin–transferrin adduct coexist in the medium [45]. This can be illustrated by Eqs. (18) and (19), in which the protein–protein adduct (Cp–$TFe^{3+}$), monoferric transferrin $TFe^{3+}$, apotransferrin and ceruloplasmin are in equilibrium. Cp′ is a ceruloplasmin species that has already transferred one $Fe^{3+}$ to T (Eq. (18)) and in which the second T1 $Cu^{2+}$ of domain 4 is available for reducing the second $Fe^{2+}$ (Eq. (19)) [29].

$$\left(Cp{-}TFe^{3+}\right) \rightleftharpoons Cp' + TFe^{3+} \tag{18}$$

$$Cp' + T \rightleftharpoons Cp'T \tag{19}$$

The experimental reciprocal relaxation times ($\tau_7^{-1}$) depend on [GSH] and 1/[$GSHFe^{2+}$]. This led us to envisage the three following possibilities (Eqs. (20)–(23)):

Possibility 1

$$GSHFe^{2+} + Cp'T \underset{k'_7}{\overset{k'_7}{\rightleftharpoons}} Cp'Fe^{3+}{-}T + GSH\,. \tag{20}$$

Possibility 2

$$Cp'Fe^{3+}{-}T \underset{k''_{-7}}{\overset{k''_7}{\rightleftharpoons}} Cp'{-}TFe^{3+}\,. \tag{21}$$

Possibility 3

$$Cp'T \underset{k_{-7}}{\overset{k_7}{\rightleftharpoons}} (Cp{-}T)' \quad (\text{rate}{-}\text{limiting}) \tag{22}$$

$$(Cp{-}T)' + GSHFe^{2+} \rightleftharpoons (Cp{-}T)'Fe^{3+} + GSH \tag{23}$$

with $K_3 = \frac{\left[(Cp-T)'Fe^{3+}\right][GSH]}{\left[(Cp-T)'\right]\left[GSHFe^{2+}\right]}$.

In Eq. (20), $Fe^{2+}$ is exchanged between $GSHFe^{2+}$ (Eq. (11)) and the protein–protein adduct. When [*GSH*], [$GSHFe^{2+}$] ≫ $c_1$, $c_2$, $c_3$, the reciprocal relaxation time equation associated with Eq. (20) can be expressed as [50]:

$$\tau_7{}'^{-1} = k'_7\left[GSHFe^{2+}\right] + k'_{-7}\left[Cp'Fe^{3+}{-}T\right]. \tag{24}$$

The experimental data do not obey Eq. (24). Eq. (20) is, therefore, rejected.

In the second possibility, after its uptake, iron is transferred from the holding site of Cp (*Cp′Fe*$^{3+}$*–T*) to T (*Cp′–TFe*$^{3+}$) in the protein–protein adduct (Eqs. (20), (21)). Under our experimental conditions, the reciprocal relaxation time equation associated with Eq. (21) is expressed as [50]:

$$\tau_7{}''^{-1} = k''_7 + k''_{-7}. \tag{25}$$

Eq. (25) is not respected by the experimental data which discounts possibility 2.

In possibility 3, $Fe^{2+}$ uptake by Cp–T is rate-limited by a change in the conformation of the protein–protein adduct (Eqs. (22), (23)). The reciprocal relaxation time equation associated with Eq. (22) is expressed as (Appendix):

$$\tau_7^{-1} = \frac{(k_7 + k_{-7})[GSH]}{K_3\left[GSHFe^{2+}\right]} + k_7. \tag{26}$$

A good linear regression is obtained for the plot of the experimental $\tau_7^{-1}$ against [*GSH*]/[$GSHFe^{2+}$] (Fig. 8). This confirms Possibility 3, by implying that the protein–protein Cp–T adduct undergoes a rate-limiting change in conformation before $Fe^{2+}$ uptake and oxidation.

*3.2.1.4. Fourth kinetic process.* At thermodynamic equilibrium, the absorption at 465 nm (Fig. 5) seems to correspond to that of a C-lobe only iron-loaded transferrin in a concentration equal to twice that of Cp ($2c_1$). The last kinetic process (Fig. 6D) lasts about 10,000 s and is detected as an exponential decrease in absorption at λ = 465 nm. It is not detected at 610 nm. Therefore, it does not involve the reduction of a T1 $Cu^{2+}$ and thereby the oxidation of $Fe^{2+}$. The experimental reciprocal relaxation times associated with this process are, within the experimental

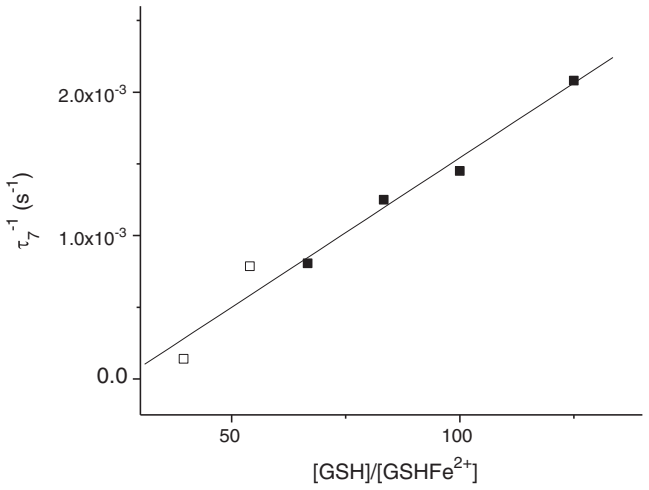


**Fig. 8.** Plot of $\tau_7^{-1}$ against [GSH]/[GSHFe$^{2+}$] with $c_1 = 2$ μM, $c_2 = 30$, 60 μM, 80 μM ≤ $c_3$ ≤ 0.15 mM, 5 mM ≤ $c_4$ ≤ 15 mM and pH 7.00. Slope, $(2.1 \pm 0.4) \times 10^{-5}$ s$^{-1}$; intercept, $(-5 \pm 5) \times 10^{-5}$ s$^{-1}$; r = 0.98307.

uncertainties and instrument stability, independent of the concentrations of the species present in the medium. They, therefore, describe a monomolecular process, such as a change in the conformation. Since the final spectrum seems to involve two C-lobe iron-loaded transferrins per ceruloplasmin, we ascribe the final kinetic phenomenon to a conformation change rate-controlling the monoferric transferrin–ceruloplasmin adduct dissociation (Eqs. (27), (28)).

$$(Cp{-}T)'Fe^{3+} \rightleftharpoons \left(Cp{-}TFe^{3+}\right) \quad (27)$$

$$\left(Cp{-}TFe^{3+}\right) \rightleftharpoons Cp'' + T_C Fe^{3+} \quad (28)$$

$$\tau_8^{-1} = k_8 + k_{-8} = (5.0 \pm 3.0)\ \text{x}\ 10^{-4}\text{s}^{-1}$$

To confirm such a possibility, we investigated the interaction of Cp with $T_CFe^{3+}$ (Eq. (29)), showed the existence of the Cp–$T_CFe^{3+}$ protein–protein adduct and measured a dissociation constant, $K_{dTcFe} = \frac{[Cp][T_C Fe^{3+}]}{[(Cp{-}T_C Fe^{3+})]}$ value of 37 ± 9 μM (Supplementary material).

$$Cp{-}T_C Fe^{3+} \rightleftharpoons Cp + T_C Fe^{3+} \quad (29)$$

This $K_{dTcFe}$ is threefold higher than the dissociation constant of Cp–T and Cp–$TFe_2$ [45], which implies that Cp–$T_CFe^{3+}$ is less stable and will dissociate more easily than two other protein–protein adducts.

## 4. Discussion

Revisiting the behavior of Cp in the presence of $Fe^{2+}$ as the sole electron-donor under anaerobic conditions was essential to analyze the possibility of an iron-transfer from Cp to T.

### 4.1. Iron(II) uptake and oxidation by ceruloplasmin

The 3D structure of Cp implies several metal-binding sites in domains 4 and 6 at 9 and 10 Å from the T1 Cu. The ligands involved in complex formation are: one imidazole of an histidine, three carboxylates of aspartate or glutamate belonging to domains 6 (H940, E935, D1025, E272) and 4 (H602, E 597, D684, E971). In the crystal structure of Cp, the sites are 50% occupied by copper. They can also complex iron and cobalt and their access is limited to small molecules [24,27,29].

We identified two iron-Cp complexes. In the first, iron acquisition and oxidation occurs with an overall dissociation constant $K_{d1} = 1$ μM (Eq. (1)) whereas, with the second, $K_{d2} = 150$ μM (Eq. (2)). This implies rather strong CpFe and weak $CpFe_2$ complexes. Moreover, the kinetic analysis allowed us to propose a multi-step mechanism for these two $Fe^{2+}$ uptakes and oxidations by Cp (Table 2).

The first process in this mechanism is detected as a sharp decrease in the absorption at 610 nm (Fig. 2A) which describes T1 $Cu^{2+}_{D6}$ reduction to T1 $Cu^{+}_{D6}$ [56]. Although $Cu^{2+}_{D6}$ reduction to $Cu^{+}_{D6}$ is responsible for the absorption decrease, it cannot occur without the electron-donor $Fe^{2+}$ which implies prior complex formation between the latter and the divalent metal-binding site of Cp situated at about 9 Å from $Cu^{2+}_{D6}$ [24,27,29]. Therefore, this absorption decrease is also related to $Fe^{2+}$ oxidation by $Cu^{2+}_{D6}$ (Eqs. (3), (4); Table 2). Indeed, complex formations with $Fe^{2+}$ and oxidation–reduction reactions are known to be extremely fast processes [55,56,61]. The divalent metal sites are common to all multicopper oxidases, and their closeness to T1 Cu should allow ultrafast electron-transfer between the two metals. This is confirmed by the kinetic and EPR experiments performed on Cp and on one of its analogs, Fet3 [55,56].

The second kinetic process (Fig. 2B) is detected by an increase in the fluorescence emission. It does not modify the absorption at 610 nm, which excludes the involvement of any reduction of T1 $Cu^{2+}$. This second phenomenon occurs in about 40 ms and describes a monomolecular process (Eq. (5), Fig. 3) during which $Fe^{3+}$ in the divalent metal-binding site probably migrates to the metal-holding site in domain 6 at the surface of the protein to yield the second kinetic product. These results imply that at the end of the second kinetic process (within 50 ms), 20% of the iron is retained in the holding site ($K_1 = 155$ μM). In the divalent binding site, $Fe^{3+}$ is coordinated to the imidazole of H940 and to the three carboxylates of E935, E272 and D1025 [24,27,29]. The carboxylate monodentates are moderately strong ligands for $Fe^{3+}$ [62], whereas imidazole is a better ligand for $Fe^{2+}$ [63]. As soon as it is oxidized, $Fe^{3+}$ can migrate to the retention site where it will be coordinated to the carboxylates of E935 and E597 in domains 6 and 4, respectively (Eq. (5); Table 2) [24,27,29].

**Table 2**
Mechanism of iron uptake and oxidation by ceruloplasmin.

| Reaction | Direct rate constant | Reverse rate constant | Equilibrium constant |
|---|---|---|---|
| $Cp + Fe^{2+} \rightleftharpoons CpFe$ (1) | | | $K_{d1} = 1.1 \pm 0.2$ μM |
| $CpFe + Fe^{2+} \rightleftharpoons CpFe_2$ (2) | | | $K_{d2} = 0.15 \pm 0.05$ mM |
| $CpCu^{2+}_{D6} + Fe^{2+} \rightleftharpoons CpCu^{2+}_{D6}Fe^{2+}$ (3) | | | $K_1 = 1.55 \times 10^{-4}$ |
| $CpCu^{2+}_{D6}Fe^{2+} \rightleftharpoons CpCu^{+}_{D6}Fe^{3+}$ (4) | | | |
| $CpCu^{+}_{D6}Fe^{3+} \underset{k_{-2}}{\overset{k_2}{\rightleftharpoons}} \{CpCu^{+}_{D6}Fe^{3+}\}$ (5) | $k_2 = (32 \pm 4)\ \text{s}^{-1}$ | $k_{-2} = (155 \pm 6)\ \text{s}^{-1}$ | $K_2 = 0.20 \pm 0.01$ |
| $(Cu^{2+}_T)CpCu^{+}_{D6}Fe^{3+} \underset{k_{-3}}{\overset{k_3}{\rightleftharpoons}} (Cu^{+}_T)CpCu^{2+}_{D6}Fe^{3+}$ (7) | $k_3 + k_{-3} = (19 \pm 3)\ \text{s}^{-1}$ | | |
| $CpCu^{2+}_{D4}(Fe^{3+}) \underset{k_{-4}}{\overset{k_4}{\rightleftharpoons}} \left\{CpCu^{2+}_{D4}(Fe^{3+})\right\}$ (8) | $k_4 + k_{-4} = (14 \pm 4) \times 10^{-3}\ \text{s}^{-1}$ | | |
| $\{CpCu^{2+}_{D4}(Fe^{3+})\} + Fe^{2+} \rightleftharpoons \{CpCu^{+}_{D4}(Fe^{3+})_2\}$ (9) | | | |

The third process (Fig. 2A, C) is detected as a fast increase (~200 ms) in the absorption at 610 nm and in fluorescence emission. It, therefore, involves the oxidation of the $Cu^{+}_{D6}$ in the second kinetic product ($Cu^{+}_{T}$) $CpCu^{2+}_{D6}Fe^{3+}$ (Eq. (7); Table 2) by one of the $Cu^{2+}_{T}$ of the trinuclear copper cluster. This oxidation is assumed to occur by an electron transfer from $Cu^{+}_{D6}$ to the trinuclear copper cluster [55,56,64]. Indeed, the oxidation–reduction potential of the T1 Cu in domain 6 is 432 mV, whereas that of each of the pair of the T3 Cu in the cluster is 482 mV [55,56,64]. This should favor electron transfer from T1 Cu to T3 Cu. Furthermore, the distance between the T1 Cu of domain 6 and the T3 Cu is about 13 Å, that between the latter and T1 Cu of domain 4 is about 27 Å, whereas that between T1 Cu of domains 6 and 4 is about 18 Å [24,29]. Consequently, electron transfer would most probably occur between the T1 Cu of domain 6 and that of the T3 Cu of the cluster [65].

The fourth slow (~200 s) process (Fig. 2D, E) is detected as a decrease in the fluorescence emission and in the absorption at 610 nm. This decrease in absorption involves the reduction of a second T1 $Cu^{2+}$. As indicated earlier, under anaerobic conditions and in the presence of $Fe^{2+}$ as the sole electron-donor, this copper reduction necessarily involves an $Fe^{2+}$ uptake prior to the electron transfer. The decrease in the fluorescence emission may also imply a change in the conformation of the protein which rate-limits this second iron uptake and oxidation. Indeed the independence of the experimental relaxation times of the concentrations of the species present in the medium confirms this proposal (Eqs. (8), (9), Table 2). As compared to other copper ferroxidases, Cp bears two additional T1 Cu in domains 2 and 4. That of domain 2 is always in the reduced state ($E^0 > 1$ V), and domain 2 does not have a second metal-binding site [29]. The role of the T1 Cu in domain 4 is not well known. However, this domain has a supplementary metal-binding site close to the T1 copper in domain 4 (T1 $Cu_{D4}$) [24,27,29]. This may explain the binding and oxidation of the second iron(II) ($K_{d2} = 150$ μM, Eq. (2)) and the fourth kinetic process (Fig. 2D, E).

### 4.2. Iron transfer from ceruloplasmin to transferrin

The presence of transferrin enhances the ferroxidase activity of Cp (Table 1). Similar enhancements were also observed in the presence of ferritin or lactoferrin which implies that Cp induces a possible acceleration of $Fe^{3+}$ uptake by these latter [66,67]. Moreover, under our experimental conditions, the main ceruloplasmin species is that interacting with T [45]. We, therefore, assumed that under similar conditions and in the presence of high concentrations of strong $Fe^{2+}$-chelating and $Fe^{3+}$-reducing agents, such as GSH [59], the addition of $Fe^{2+}$ would imply the uptake and the oxidation of the metal by the CpT protein–protein adduct, and its eventual transfer from Cp to T. This allows us to propose a multistep mechanism for $Fe^{3+}$ transfer from Cp to T (Table 3). It should be added here that GSH is universally present in biological media and was recently assumed to function as the labile cytosolic iron pool [58].

very fast 1st complex formation — rate-limiting conformation changes

$$T_C\text{-}T_N + 2Fe^{3+} \underset{<1\ s}{\rightleftharpoons} T_CFe\text{-}T_N + Fe^{3+} \underset{500\ s}{\rightleftharpoons} \text{kinetic products} \underset{\sim 4000\ s}{\rightleftharpoons} TFe_2$$

**Scheme I.** The mechanism of $Fe^{3+}$ uptake by transferrin.

Apotransferrin is in an open conformation. When it becomes iron-loaded, both C- and N-lobes transit from an open to a closed conformation where iron is totally protected from the bulk [34,68]. Moreover, the affinity of the C-lobe for $Fe^{3+}$ is one order of magnitude higher than that of the N-lobe [69,70]. In the case of iron(III) uptake by free apotransferrin from rapidly dissociating chelates, such as iron nitrilotriacetate or iron trisacetohydroxamato, $Fe^{3+}$ is rapidly (<1 s) transferred from the chelates to the C-lobe to form a first complex with the phenates of the tyrosine ligands. This induces a series of proton transfers affecting the histidine ligand and rate-limited by conformation changes, the slowest (4000 s) of which controls iron uptake by the N-lobe [41,42]. When a single iron is available per transferrin, the same changes in conformation also occur to yield the monoferric C-lobe-only iron-loaded transferrin, (Scheme I) [41,42] where $T_C$ and $T_N$ are the C- and N-lobes of transferrin, respectively.

This cooperativity between the C- and N-lobes implies that the N-lobe cannot be iron-loaded before the C-lobe. Furthermore, $T_CFe$–$T_N$ is recognized by transferrin receptor 1 with affinities similar to that for holotransferrin. Thus, $T_CFe$–$T_N$ also delivers iron by the major iron-acquisition pathway [46,71].

Four kinetic processes are detected when $GSHFe^{2+}$ is mixed with a solution of T and Cp. The first (~100 s, Fig. 7) leads to the emergence of an absorption band at $\lambda_{max} = 477$ nm (Fig. 5). This absorption band is not observed with T and $Fe^{2+}$ in the absence of Cp. Neither can it be ascribed to the $Fe^{3+}$ complex with the phenates of the tyrosines in the free iron-loaded transferrin, which has an absorption maximum of 465 nm [41,42]. Furthermore, the kinetic process of Fig. 6A is much too slow to describe $Fe^{2+}$ uptake and oxidation by Cp, which occurs in less than 1 s (Eqs. (4), (5); Table 2, Fig. 2A). It is also much too fast to be related to iron uptake by the N-site of transferrin (Scheme I) [41,42]. Subsequently, we are dealing here with a $Fe^{3+}$ transfer from the holding site of Cp in domain 6 to the C-lobe of transferrin in interaction with ceruloplasmin (Eq. (12), Table 3). This explains the emergence of the 477 nm band, and is confirmed by the amplitude of the first absorbance decrease at 610 nm in Fig. 5 which is typical of T1 $Cu^{2+}$ reduction. This amplitude is much too low to involve more than one T1 $Cu^{2+}$ in the process and, thereby, more than one $Fe^{2+}$ oxidation.

This monomolecular $Fe^{3+}$ transfer from Cp to T is followed by a second kinetic process, detected in the 500 s range as an increase in the absorptions at 610 and 477 nm (Fig. 6B, C). The first is typical of the re-oxidation of $Cu^{+}_{D6}$ by one $Cu^{2+}$ of the trinuclear cluster. This process is extremely fast in the absence of T (Fig. 2A, B). It seems, therefore, to be rate-limited by a conformation change in the Cp–$TFe^{3+}$ adduct (Eq. (16), Table 3). It is, moreover, accompanied by a hypsochromic

**Table 3**
Mechanism of iron transfer from ceruloplasmin to transferrin.

| Reaction | Rate constants | Equilibrium constant |
|---|---|---|
| $Cp + T \rightleftharpoons Cp - T$ | | $19 \pm 7$ μM |
| $Cp + T_CFe^{3+} \rightleftharpoons Cp - T_CFe^{3+}$ (29) | | $37 \pm 9$ μM |
| $CpFe^{3+}\text{–}T \underset{k_{-5}}{\overset{k_5}{\rightleftharpoons}} Cp\text{–}TFe^{3+}$ (12) | $k_5 + k_{-5} = (2.2 \pm 0.2) \times 10^{-2}\ s^{-1}$ | |
| $Cp\text{–}TFe^{3+} \underset{k_{-6}}{\overset{k_6}{\rightleftharpoons}} (Cp\text{–}TFe^{3+})$ (16) | $k_6 + k_{-6} = (8.0 \pm 1.4) \times 10^{-3}\ s^{-1}$ | |
| $(Cp - TFe^{3+}) \rightleftharpoons Cp' + TFe^{3+}$ (18) | | |
| $Cp' + T \rightleftharpoons Cp'\,T$ (19) | | |
| $Cp'T \underset{k_{-7}}{\overset{k_7}{\rightleftharpoons}} (Cp\text{–}T)'$ (22) | | |
| $(Cp - T)' + GSHFe^{2+} \rightleftharpoons (Cp - T)'\,Fe^{3+} + GSH$ (23) | | |
| $(Cp\text{–}T)'Fe^{3+} \underset{k_{-8}}{\overset{k_8}{\rightleftharpoons}} Cp\text{–}TFe^{3+}$ (27) | $k_8 + k_{-8} = (5.0 \pm 3.0) \times 10^{-4}\ s^{-1}$ | |

shift of the absorption from 477 to 465 nm. The absorption maximum at 465 nm is typical of $T_CFe–T_N$ (Scheme I) [41,42]. The third process is only detected as a slow (3000 s) decrease in the absorption at 610 nm (Fig. 6C). It, therefore, implies $Cu^{2+}$ reduction and $Fe^{2+}$ oxidation. It is not observed at 465 nm and does not, therefore, concern any $Fe^{3+}$ transfer from Cp to T. It is, moreover, a monomolecular process that rate-limits a second $Fe^{2+}$ uptake and oxidation by Cp in the protein–protein adduct to yield a third kinetic product, in which $Fe^{3+}$ is probably held in the labile site of domain 4 in Cp (Eqs. (22), (23); Table 3).

The fourth kinetic process is very slow (10,000 s). It shows a decrease in the absorption at 465 nm and is not detected at 610 nm. It does not, therefore, involve any oxidation–reduction of T1 $Cu^{2+}$. At the end of this monomolecular kinetic process, the absorption spectra are typical of two monoferric C-lobe iron-loaded transferrins [42] per ceruloplasmin. We ascribe this last phenomenon to a change in conformation which allows the dissociation of the Cp–$T_CFe^{3+}$ adduct (Eqs. (27), (28); Table 3).

Under our anaerobic experimental conditions, the only $Fe^{3+}$ available for apotransferrin is that provided by $Fe^{2+}$ oxidation by Cp. Therefore, its concentration cannot exceed twice that of Cp, which is much lower than that of apotransferrin ($c_1 \ll c_2$). This excludes $Fe^{3+}$ uptake by the N-lobe of free apotransferrin [41,42]. However, this does not eliminate the involvement of the N-lobe of the apotransferrin in interaction with Cp in the uptake of $Fe^{3+}$. A recent hybridization study concerning lactoferrin (Lf) with Cp suggests an interaction of the N-lobe of Lf with Cp [72]. In this proposal, Cp captures $Fe^{2+}$, oxidizes it and directly transfers it to the N-lobe of Lf [72]. However, in this model, the C-lobe of Lf is in the closed conformation. More recently, small-angle X-ray scattering experiments were not able to discriminate between the involvement of either the N- or C-lobes of Lf in its interaction with Cp [73]. Therefore, with regards to the structural similarities between the C- and N-lobes of both Lf and T, the C-lobe of T in its open conformation probably interacts with Cp. On the other hand, experiments of the incorporation $Fe^{3+}$ by T after $Fe^{2+}$ oxidation by a recombinant of hephaestine (a transmembrane ferroxidase homologue of Cp) show that within 60 min, only the C-lobe of transferrin is iron-loaded. Holotransferrin starts appearing in more than 2 h [74]. Another copper ferroxidase, Fox1, in *Chlamydomonas reinhardtii* mainly catalyzes $T_CFe^{3+}$ formation [75].

We recently identified Cp–T and Cp–$TFe_2$ protein–protein adducts, found average dissociation constants of about 15 μM for both the apotransferrin- and holotransferrin–ceruloplasmin complexes [45]. We report here a dissociation constant of 37 μM for Cp–$T_CFe^{3+}$ (Supplementary material). This implies that the latter is thermodynamically less favored than Cp–T and Cp–$TFe_2$. From a statistical standpoint and under our experimental conditions, the scarcity of the $Fe^{3+}$-loaded transferrin (which cannot exceed $2c_1$) as compared to that of free apotransferrin ($c_2$ ~ 15–150 $c_1$) largely favors the ceruloplasmin–apotransferrin complex. This and the spectra of the final thermodynamic product in Fig. 5 lead us to envisage an equilibrium between $T_CFe^{3+}$, Cp and the protein–protein adducts (Eqs. (27), (28), Table 3). Furthermore, this does not support, under our experimental conditions, the hypothesis of a possible $Fe^{2+}$ oxidation in an eventual $Fe^{2+}$–transferrin complex [10]. The affinity of transferrin for $Fe^{3+}$ (~$10^{21}$) is at least 14 orders of magnitude higher than that for $Fe^{2+}$ [36]. Therefore, no competition occurs between $Fe^{2+}$ and $Fe^{3+}$ towards complex formation with transferrin and all the $Fe^{3+}$ obtainable from Cp is complexed by transferrin as shown in Fig. 5. This does not imply the absence of a $Fe^{2+}$–transferrin complex in the medium. It shows, however, that, if this complex exists, it cannot, at least under our experimental conditions, be involved in $Fe^{2+}$ oxidation.

Our kinetic analysis clearly indicates that after $Fe^{2+}$ uptake and its oxidation to $Fe^{3+}$, the metal is transferred from Cp to T in Cp–T. This is also observed in yeast and in *C. reinhardtii*, where a direct transfer of iron occurs from the ferroxidases, Fet3, and Fox1, to the iron transport, Ftr1 [75,76].

Although unlikely, the extraction of $Fe^{3+}$ from the holding site of Cp by a low molecular-weight-chelator and its transfer from the chelate to T remains possible. The most eligible candidate for such a purpose would probably be citrate [77,78]. However, complex formation between the citrate present in biological fluids and $Fe^{3+}$ should not be very efficient, because of the low concentrations of non-transferrin-bound iron (<0.5 μM) and the very low rates of $Fe^{3+}$ transfer from the citrate complex to apotransferrin (>20 h) [79]. This would be much less productive than a direct transfer from Cp to T, which occurs for the first iron in about 100 s (Fig. 7, Eq. (12), Table 3). Molecular interactions between proteins can be very fast [80]. Therefore, the rather high dissociation constants of Cp–$TFe_2$ and Cp–T and the high affinity of holo- and monoferric transferrin for receptor 1 render these iron-loaded species readily available for endocytosis.

## 5. Conclusion

Iron in its two major oxidation states cannot freely exist in a biological fluid. Its acquisition as $Fe^{2+}$ and transport as $Fe^{3+}$ should, therefore, be dealt with in compartments isolated from the environmental neutral biological medium. Cp and T seem to play this role, which requires at least three essential conditions. The first concerns $Fe^{2+}$ uptake by the divalent metallic sites of Cp, its oxidation and its transfer to the holding sites near the surface of the protein. The second should imply the existence of a protein–protein adduct between Cp and T. The third should allow $Fe^{3+}$ transfer from the holding site of the Cp–T adduct to the binding sites of transferrin. We show here that these three conditions are fulfilled in vitro.

## Acknowledgements

The authors are grateful to Dr J. S. Lomas for helpful discussions and for the Lebanese National Council of Scientific Research for C. Eid PhD Grant.

## References

[1] P. Aisen, C. Enns, M. Wessling-Resnick, Chemistry and biology of eukaryotic iron metabolism, Int. J. Biochem. Cell Biol. 33 (2001) 940–959.
[2] R. Crichton, Iron Metabolism from Molecular Mechanisms to Clinical Consequences, 3rd ed. J. Wiley, Chichester, 2009.
[3] J.M. El Hage Chahine, M. Hemadi, N.T. Ha-Duong, Uptake and release of metal ions by transferrin and interaction with receptor 1, Biochim. Biophys. Acta 1820 (2012) 334–347.
[4] M. Khalil, T. C., L. C., Iron and neurodegeneration in multiple sclerosis, Mult. Scler. Int. 606807 (2011).
[5] F. Krötz, H.Y. Sohn, U. Pohl, Reactive oxygen species players in the platelet game, Arterioscler. Thromb. Vasc. Biol. 24 (2004) 1988–1996.
[6] H.P. Roeser, G.R. Lee, S. Nacht, G.E. Cartwright, The role of ceruloplasmin in iron metabolism, J. Clin. Invest. 49 (1970) 2408–2417.
[7] E. Frieden, Ceruloplasmin, a link between copper and iron metabolism, Ortop. Travmatol. Protez. 30 (1969) 87–91.
[8] S. Osaki, D.A. Johnson, E. Frieden, The possible significance of the ferrous oxidase activity of ceruloplasmin in normal human serum, J. Biol. Chem. 241 (1966) 2746–2751.
[9] J.A. McDermott, C.T. Huber, S. Osaki, E. Frieden, Role of iron in the oxidase activity of ceruloplasmin, Biochim. Biophys. Acta 151 (1968) 541–557.
[10] S. Dhungana, C.H. Taboy, O. Zak, M. Larvie, A.L. Crumbliss, P. Aisen, Redox properties of human transferrin bound to its receptor, Biochemistry 43 (2004) 205–209.
[11] E.D. Harris, Copper transport: an overview, Proc. Soc. Exp. Biol. Med. (1991) 130–140.
[12] E. Frieden, H.S. Hsieh, Ceruloplasmin: the copper transport protein with essential oxidase activity, Adv. Enzymol. Relat. Areas Mol. Biol. 44 (1976) 187–236.
[13] N.E. Hellman, J.D. Gitlin, Ceruloplasmin metabolism and function, Annu. Rev. Nutr. 22 (2002) 439–458.
[14] R. Wever, F.X. van Leeuwen, B.F. van Gelder, The reaction of nitric oxide with ceruloplasmin, Biochim. Biophys. Acta 302 (1973) 236–239.
[15] J. Torres, M.T. Wilson, The reactions of copper proteins with nitric oxide, Biochim. Biophys. Acta 1411 (1999) 310–322.
[16] S.Y. Jeong, S. David, Glycosylphosphatidylinositol-anchored ceruloplasmin is required for iron efflux from cells in the central nervous system, J. Biol. Chem. 278 (2003) 27144–27148.
[17] H.A. Ragan, S. Nacht, G.R. Lee, C.R. Bishop, G.E. Cartwright, Effect of ceruloplasmin on plasma iron in copper-deficient swine, Am. J. Physiol. 217 (1969) 1320–1323.
[18] S. Osaki, D.A. Johnson, Mobilization of liver iron by ferroxidase (ceruloplasmin), J. Biol. Chem. 244 (1969) 5757–5758.

[19] X. Xu, S. Pin, M. Gathinji, R. Fuchs, Z.L. Harris, Aceruloplasminemia: an inherited neurodegenerative disease with impairment of iron homeostasis, Ann. N. Y. Acad. Sci. 1012 (2004) 299–305.
[20] Z.L. Harris, A.P. Durley, T.K. Man, J.D. Gitlin, Targeted gene disruption reveals an essential role for ceruloplasmin in cellular iron efflux, Proc. Natl. Acad. Sci. U. S. A. 96 (1999) 10812–10817.
[21] L.A. Meyer, A.P. Durley, J.R. Prohaska, Z.L. Harris, Copper transport and metabolism are normal in aceruloplasminemic mice, J. Biol. Chem. 276 (2001) 36857–36861.
[22] T.L. Ortel, N. Takahashi, F.W. Putnam, Structural model of human ceruloplasmin based on internal triplication, hydrophilic/hydrophobic character, and secondary structure of domains, Proc. Natl. Acad. Sci. U. S. A. 81 (1984) 4761–4765.
[23] N. Takahashi, T.L. Ortel, F.W. Putnam, Single-chain structure of human ceruloplasmin: the complete amino acid sequence of the whole molecule, Proc. Natl. Acad. Sci. U. S. A. 81 (1984) 390–394.
[24] P.F. Lindley, G. Card, I. Zaitseva, V. Zaitsev, B. Reinhammar, E. Selin-Lindgren, K. Yoshida, An X-ray structural study of human ceruloplasmin in relation to ferroxidase activity, J. Biol. Inorg. Chem. 2 (1997) 454–463.
[25] D.J. Kosman, Multicopper oxidases: a workshop on copper coordination chemistry, electron transfer, and metallophysiology, J. Biol. Inorg. Chem. 15 (2010) 15–28.
[26] E.I. Solomon, U.M. Sundaram, T.E. Machonkin, Multicopper oxidases and oxygenases, Chem. Rev. 96 (1996) 2563–2606.
[27] V.N. Zaitsev, I. Zaitseva, M. Papiz, P.F. Lindley, An X-ray crystallographic study of the binding sites of the azide inhibitor and organic substrates to ceruloplasmin, a multi-copper oxidase in the plasma, J. Biol. Inorg. Chem. 4 (1999) 579–587.
[28] L. Calabrese, M. Carbonaro, G. Musci, Presence of coupled trinuclear copper cluster in mammalian ceruloplasmin is essential for efficient electron transfer to oxygen, J. Biol. Chem. 264 (1989) 6183–6187.
[29] I. Bento, C. Peixoto, V.N. Zaitsev, P.F. Lindley, Ceruloplasmin revisited: structural and functional roles of various metal cation-binding sites, Acta Crystallogr. D Biol. Crystallogr. 63 (2007) 240–248.
[30] O. Farver, L. Bendahl, L.K. Skov, I. Pecht, Human ceruloplasmin. Intramolecular electron transfer kinetics and equilibration, J. Biol. Chem. 274 (1999) 26135–26140.
[31] G. Musci, G.C. Bellenchi, L. Calabrese, The multifunctional oxidase activity of ceruloplasmin as revealed by anion binding studies, Eur. J. Biochem. 265 (1999) 589–597.
[32] A.S. Moore, B.F. Anderson, C.R. Groom, M. Haridas, E.N. Baker, Three-dimensional structure of diferric bovine lactoferrin at 2.8 Å resolution, J. Mol. Biol. 274 (1997) 222–2236.
[33] J. Wally, P.J. Halbrooks, C. Vonrhein, M.A. Rould, S.J. Everse, M.A. B., S.K. Buchanan, The crystal structure of iron-free from human serum transferrin provides insight into inter-lobe communication and receptor binding, J. Biol. Chem. 281 (2006) 24934–24944.
[34] H.J. Zuccola, The Crystal Structure of Monoferric Human Serum Transferrin, (Ph.D. Thesis) Georgia Institute of Technology, UMI, Ann Arbor, 1992.
[35] P. Aisen, A. Leibman, J. Zweier, Stochiometric and site characteristics of the binding of iron to human transferrin, J. Biol. Chem. 253 (1978) 1930–1937.
[36] W.R. Harris, Estimation of the ferrous-transferrin binding constants based on thermodynamic studies of nickel(II)-transferrin, J. Inorg. Biochem. 27 (1986) 41–52.
[37] M. Hémadi, P.H. Kahn, G. Miquel, J.M. El Hage Chahine, Transferrin's mechanism of interaction with receptor 1, Biochemistry 43 (2004) 1736–1745.
[38] A. Dautry-Varsat, A. Ciechanover, H.F. Lodish, pH and the recycling of transferrin during receptor-mediated endocytosis, Proc. Natl. Acad. Sci. U. S. A. 80 (1983) 2258–2262.
[39] P. Aisen, Transferrin metabolism and the liver, Semin. Liver Dis. 4 (1984) 193–206.
[40] P. Aisen, Transferrin, the transferrin receptor, and the uptake of iron by cells, Met. Ions Biol. Syst. 35 (1998) 585–631.
[41] R. Pakdaman, F.B. Abdallah, J.M. El Hage Chahine, Transferrin, is a mixed chelate–protein ternary complex involved in the mechanism of iron uptake by serum-transferrin in vitro? J. Mol. Biol. 293 (1999) 1273–1284.
[42] R. Pakdaman, J.M. El Hage Chahine, A mechanism for iron uptake by transferrin, Eur. J. Biochem. 236 (1996) 922–931.
[43] D. Darbari, M. Loyevsky, V. Gordeuk, J.A. Kark, O. Castro, S. Rana, V. Apprey, J. Kurantsin-Mills, Fluorescence measurements of the labile iron pool of sickle erythrocytes, Blood 102 (2003) 357–364.
[44] Y. Ma, Z. Liu, R.C. Hider, F. Petrat, Determination of the labile iron pool of human lymphocytes using the fluorescent probe, CP655, Anal. Chem. Insights 2 (2007) 61–67.
[45] N.T. Ha-Duong, C. Eid, M. Hemadi, J.M. El Hage Chahine, In vitro interaction between ceruloplasmin and human serum transferrin, Biochemistry 49 (2010) 10261–10263.
[46] M. Hémadi, G. Miquel, P.H. Kahn, J.M. El Hage Chahine, Aluminum exchange between citrate and human serum transferrin and interaction with transferrin receptor 1, Biochemistry 42 (2003) 3120–3130.
[47] E.D. Weinberg, Iron and infection, Microbiol. Rev. 42 (1978) 45–66.
[48] A.G. Morell, C.J. Van den Hamer, I.H. Scheinberg, Physical and chemical studies on ceruloplasmin. VI. Preparation of human ceruloplasmin crystals, J. Biol. Chem. 244 (1969) 3494–3496.
[49] M. Eigen, L. DeMaeyer, Relaxation methods, in: S.L. Friess, E.S. Lewis, A. Weissberger (Eds.), Techniques of Organic Chemistry — Investigation of Rates and Mechanism of Reactions, part II, vol. 8, Wiley Intersciences, New York, 1963, pp. 895–1029.
[50] C.F. Bernasconi, Relaxation Kinetics, Academic Press, New-York, 1976.
[51] P.M. Hanna, R. Tamilarasan, D.R. McMillin, Cu(I) analysis of blue copper proteins, Biochem. J. 256 (1988) 1001–1004.
[52] E.T. Zakharova, M.M. Shavlovski, M.G. Bass, A.A. Gridasova, M.O. Pulina, V. De Filippis, M. Beltramini, P. Di Muro, B. Salvato, A. Fontana, V.B. Vasilyev, V.S. Gaitskhoki, Interaction of lactoferrin with ceruloplasmin, Arch. Biochem. Biophys. 374 (2000) 222–228.
[53] M.E. Van Eden, S.D. Aust, Intact human ceruloplasmin is required for the incorporation of iron into human ferritin, Arch. Biochem. Biophys. 381 (2000) 119–126.
[54] R. Binstead, A. Zuberbuhler, B. Jung, SPECFIT Global Analysis System Version 3.04.34, 2003.
[55] T.E. Machonkin, L. Quintanar, A.E. Palmer, R. Hassett, S. Severance, D.J. Kosman, E.I. Solomon, Spectroscopy and reactivity of the type 1 copper site in Fet3p from *Saccharomyces cerevisiae*: correlation of structure with reactivity in the multicopper oxidases, J. Am. Chem. Soc. 123 (2001) 5507–5517.
[56] T.E. Machonkin, E.I. Solomon, The thermodynamics, kinetics, and molecular mechanism of intramolecular electron transfer in human ceruloplasmin, J. Am. Chem. Soc. 122 (2000) 12547–12560.
[57] M. Eigen, L. DeMaeyer, Techniques of Chemistry, Wiley, New York, 1973.
[58] R.C. Hider, X. Kong, Iron speciation in the cytosol: an overview, Dalton Trans. 42 (2013) 3220–3229.
[59] R.C. Hider, X.L. Kong, Glutathione: a key component of the cytoplasmic labile iron pool, Biometals 24 (2011) 1179–1187.
[60] S. Osaki, Kinetic studies of ferrous ion oxidation with crystalline human ferroxidase (ceruloplasmin), J. Biol. Chem. 241 (1966) 5053–5059.
[61] M. Eigen, R.G. Wilkins, The Kinetics and Mechanism of Formation of Metal Complexes, Advances in Chemistry, Buffalo, N. Y. 1965.
[62] H. Tsubota, Formation constants of some metal formate complexes, and the use of formate buffer solution as an elutriant for cation-exchange chromatography, Bull. Soc. Chem. Japan 35 (1962) 640–644.
[63] R.G. Pearson, Hard and Soft Acids and Bases, Dowden, Hutchinson and Ross, Strasbourg, 1973.
[64] T.E. Machonkin, H.H. Zhang, B. Hedman, K.O. Hodgson, E.I. Solomon, Spectroscopic and magnetic studies of human ceruloplasmin: identification of a redox-inactive reduced Type 1 copper site, Biochemistry 37 (1998) 9570–9578.
[65] L. Quintanar, M. Gebhard, T.P. Wang, D.J. Kosman, E.I. Solomon, Ferrous binding to the multicopper oxidases *Saccharomyces cerevisiae* Fet3p and human ceruloplasmin: contributions to ferroxidase activity, J. Am. Chem. Soc. 126 (2004) 6579–6589.
[66] S.H. Juan, S.D. Aust, Studies on the interaction between ferritin and ceruloplasmin, Arch. Biochem. Biophys. 355 (1998) 56–62.
[67] C.A. Reilly, S.D. Aust, Stimulation of the ferroxidase activity of ceruloplasmin during iron loading into ferritin, Arch. Biochem. Biophys. 347 (1997) 242–248.
[68] J. Wally, S.K. Buchanan, A structural comparison of human serum transferrin and human lactoferrin, Biometals 20 (2007) 249–262.
[69] P. Aisen, Physical biochemistry of the transferrins — update 1984–1988, in: T.M. Loehr, H.B. Gray, A.B.P. Lever (Eds.), Iron Carriers and Proteins, vol. 5, V.C.H. Publishers, N. Y., 1989, pp. 353–371.
[70] P. Aisen, E.B. Brown, The iron-binding function of transferrin in iron metabolism, Semin. Hematol. 14 (1977) 31–53.
[71] M. Hémadi, N.T. Ha-Duong, J.M. El Hage Chahine, The mechanism of iron release from the transferrin-receptor 1 adduct, J. Mol. Biol. 358 (2006) 1125–1136.
[72] K.N. White, C. Conesa, L. Sanchez, M. Amini, S. Farnaud, C. Lorvoralak, R.W. Evans, The transfer of iron between ceruloplasmin and transferrins, Biochim. Biophys. Acta 1820 (2012) 411–416.
[73] V.R. Samygina, A.V. Sokolov, G. Bourenkov, M.V. Petoukhov, M.O. Pulina, E.T. Zakharova, V.B. Vasilyev, H. Bartunik, D.I. Svergun, Ceruloplasmin: macromolecular assemblies with iron-containing acute phase proteins, PLoS One 8 (2013) e67145.
[74] T.A. Griffiths, A.G. Mauk, R.T. MacGillivray, Recombinant expression and functional characterization of human hephaestin: a multicopper oxidase with ferroxidase activity, Biochemistry 44 (2005) 14725–14731.
[75] A. Terzulli, D.J. Kosman, Analysis of the high-affinity iron uptake system at the *Chlamydomonas reinhardtii* plasma membrane, Eukaryot. Cell 9 (2010) 815–826.
[76] E.Y. Kwok, S. Severance, D.J. Kosman, Evidence for iron channeling in the Fet3p–Ftr1p high-affinity iron uptake complex in the yeast plasma membrane, Biochemistry 45 (2006) 6317–6327.
[77] R.C. Hider, A.M. Silva, M. Podinovskaia, Y. Ma, Monitoring the efficiency of iron chelation therapy: the potential of nontransferrin-bound iron, Ann. N. Y. Acad. Sci. 1202 (2010) 94–99.
[78] M. Grootveld, J.D. Bell, B. Halliwell, O.I. Aruoma, A. Bomford, P.J. Sadler, Non-transferrin-bound iron in plasma or serum from patients with idiopathic hemochromatosis. Characterization by high performance liquid chromatography and nuclear magnetic resonance spectroscopy, J. Biol. Chem. 264 (1989) 4417–4422.
[79] G.W. Bates, C. Billups, P. Saltman, The kinetics and mechanism of iron(III) exchange between chelates and transferrin. I. The complexes of citrate and nitrilotriacetic acid, J. Biol. Chem. 242 (1967) 2810–2815.
[80] Z. Chikh, M. Hemadi, G. Miquel, N.T. Ha-Duong, J.M. El Hage Chahine, Cobalt and the iron acquisition pathway: competition towards interaction with receptor 1, J. Mol. Biol. 380 (2008) 900–916.